Supplement of Atmos. Meas. Tech., 17, 6119–6144, 2024
https://doi.org/10.5194/amt-17-6119-2024-supplement

Atmospheric Measurement Techniques
Open Access
EGU

Supplement of

ALICENET – an Italian network of automated lidar ceilometers for four-dimensional aerosol monitoring: infrastructure, data processing, and applications

Annachiara Bellini et al.

Correspondence to: Annachiara Bellini (a.bellini@arpa.vda.it) and Francesca Barnaba (francesca.barnaba@cnr.it)

S1 Cloud screening

To avoid contamination of aerosol retrievals by clouds and droplets, the ALC signal is filtered out from 500 m below the Cloud Base Height (CBH) and above. The CBH provided by the ALC firmware is used for this purpose. This additional 500 m-buffer was conservatively chosen to limit the impact of variability in the CBH identification due to differences in instrument type and firmware version. A temporal cloud filter is also applied, removing signals collected 15 minutes before to 15 minutes after the firmware cloud detection, using the same criteria as above.

As an example of the effect of the cloud screening procedure, Fig. S1 shows three different cloud-affected, 1-hour averaged total attenuated backscatter profiles before (black line) and after (blue line) the cloud-screening. These ALC measurements were collected in Aosta in the presence of low (Fig. S1a), medium (Fig. S1b), and high (Fig. S1c) clouds.

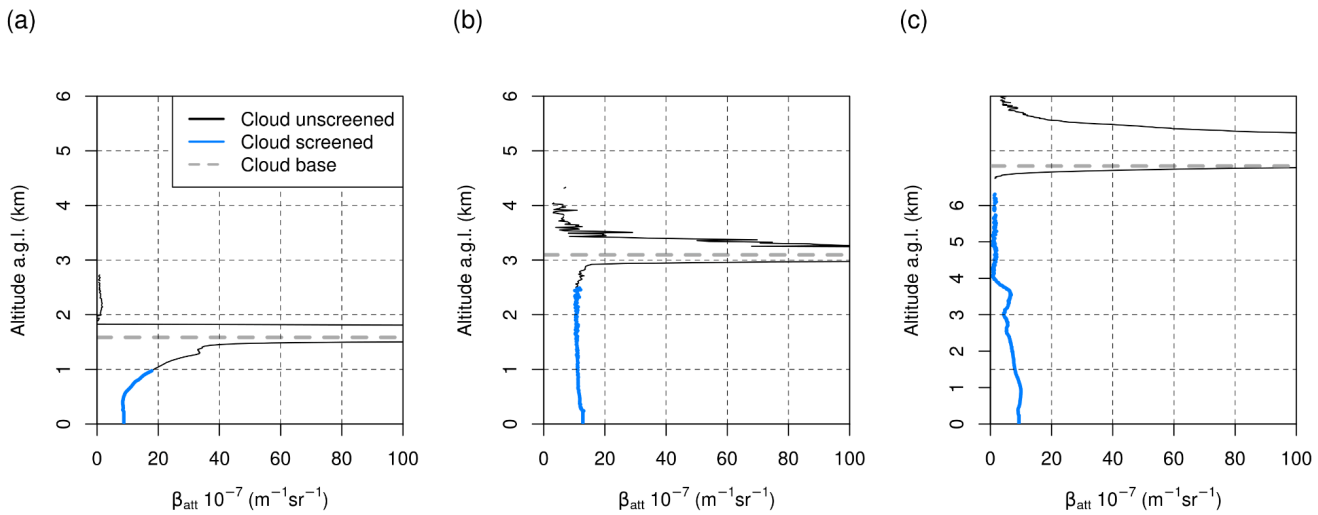

Figure S1: Examples of the ALICENET cloud unscreened (black line) and cloud screened (blue line) total attenuated backscatter (β_{att}) profiles derived from the CHM15k signals in Aosta: (a) 19/06/2022 4-5 UTC, (b) 27/06/2022 11-12 UTC, (c) 18/06/2022 20-21 UTC. The x-axis was cut at 100 m^{-1} sr^{-1} to highlight the aerosol profile better. The cloud base heights identified by the ALC firmware are also reported (dashed line). Both β_{att} profiles and cloud base heights are 1-hour averaged.

S2 Overlap correction

The derivation of the overlap correction to be applied to the ALICENET CHM15k systems is based on the procedure of Hervo et al. (2016), plus additional quality controls (QC.OVL, see also Table S1 in supplement S6). The Hervo procedure selects time windows in which a nearly homogeneous aerosol layer can be assumed in the first 1200 m. Then, based on this homogeneity assumption, for each selected time window it derives an overlap correction factor, $f_c(r)$, to be applied to the overlap correction function provided by the manufacturer, $Ovl_{man}(r)$, so that the new overlap correction function is:

$$Ovl(r) = \frac{Ovl_{man}(r)}{f_c(r)} \quad \text{(S1)}$$

The relative difference (RD) between the Ovl-corrected and the Ovl_{man}-corrected ALC signals is thus $RD(r) = f_c(r) - 1$.

As Hervo et al. (2016) found, fc(r) depends on the system's internal temperature, which exhibits a seasonal cycle. To account for this dependence, an ensemble of $f_c(r)$ is derived using an ALC dataset spanning different seasons. Each $f_c(r)$ is related through a linear fit with the system's internal temperature (T_{instr}) within the corresponding time window. This procedure gives a system-, range- and temperature-dependent 'overlap model' $Ovl_{model}(r,T)$.

Since the assumption of aerosol homogeneity in the lowermost levels is particularly critical at some ALICENET stations, we introduced specific quality controls to derive a robust $Ovl_{model}(r,T)$ for systems operating at each site:

a) before the derivation of the overlap model, a filter (QC.OVL1) is applied to the ensemble of overlap correction factors to reject those likely derived in inhomogeneous conditions, thus leading to unrealistic overlap corrections. Operationally, for each $f_c(r)$ the following metric is calculated:

$$M_{ov} = \sum \frac{\left(\frac{median\left(\left|RD(r) - RD_i(r)\right|\right)}{\left|T_{instr} - T_i\right|} \right)}{N} \quad \text{(S2)}$$

where RD and T_{instr} are the relative difference and the system internal temperature associated with the considered $f_c(r)$, the median is calculated over the vertical range 225-1200 m. The sum is performed over the sub-ensemble of N system internal temperatures T_i and associated relative differences RD_i lying between ± 5 K from the T_{instr}. Then, those $f_c(r)$ associated with $M_{ov} < 0.05$ are rejected;

b) the number of non-rejected overlap correction factors must be > 20 (QC.OVL2);

c) an ALC dataset longer than nine months must be used to obtain a statistically significant ensemble of overlap functions spanning a representative range of temperature (QC.OVL3);

If the above QCs are met, the overlap model is derived using a robust linear fit (rlm R package).

Fig. S2 shows examples of the relative differences between the ALC signals as corrected with the ALICENET QC overlap models and the manufacturer overlap functions, referring to the Rome and Aosta CHM15k systems.

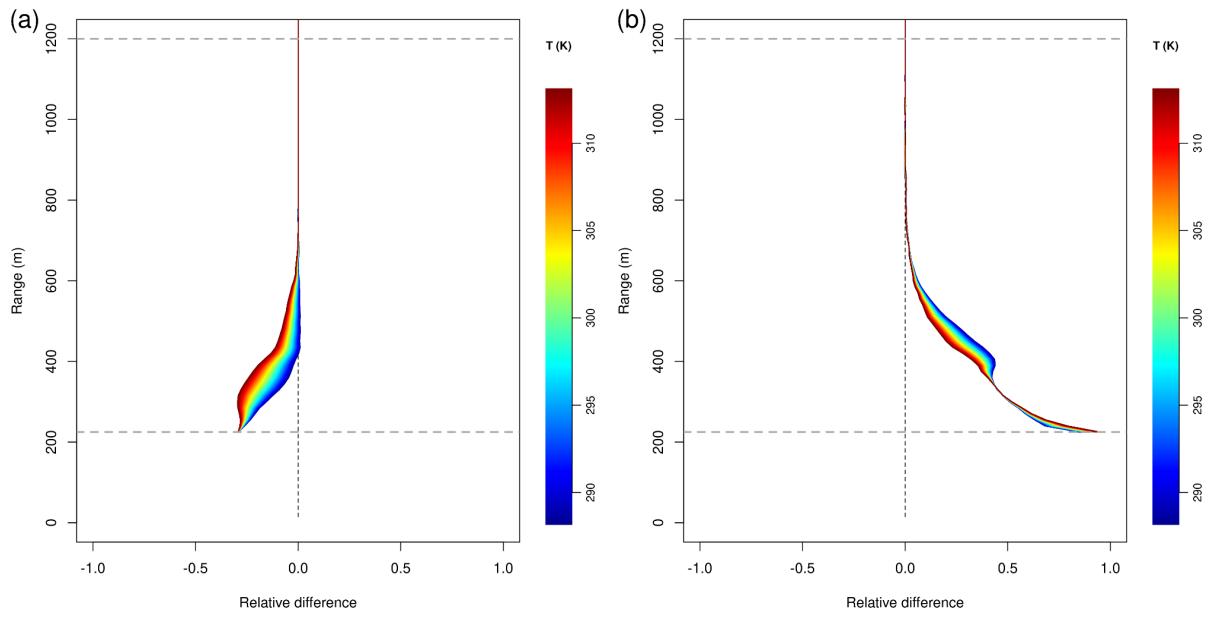

Figure S2: Range- (y axis) and temperature- (colour) dependent relative differences (RD) between the ALC signals corrected using the quality-controlled overlap models derived by ALICENET and the manufacturer overlap functions. The two plots refer to the overlap corrections applied to the CHM15k systems in (a) Rome, and (b) Aosta.

To avoid altitude ranges where the partial overlap is still insufficient to derive quantitative information, the overlap correction is only applied down to a 225 m altitude a.g.l. Below this altitude, the raw profiles are extrapolated down to the ground by linear fitting in winter (using data from 225 m to 285 m) or assuming a homogeneous profile below 225 m in summer.

S3 Absolute calibration

The Rayleigh calibration procedure implemented in ALICENET is based on comparing the pre-processed ALC signal with a theoretical molecular profile in aerosol-free regions. The theoretical molecular backscatter profile at the operating wavelength is derived using the Bodhaine formulation (Bodhaine, 1999) and site- and monthly-dependent temperature and pressure profiles extracted from ERA5 reanalyses. The procedure comprises two steps: a) selection of the optimal molecular window for calibration, and b) computation of the calibration coefficient C_L. Each step includes specific quality controls (QC.CAL, see also Table S1 in supplement S6).

a) The selection of the molecular window is performed considering nighttime-only profiles to avoid sunlight noise and using vertical profiles collected over 3–6 hours, depending on cloudiness, and between 3-7 km a.g.l. Along this vertical range, an iterative procedure is applied over an ensemble of 'potential' molecular windows centred at different altitudes and with variable amplitudes, ranging from 600 to 3000 m at steps of 30 m. For each potential range window, i.e., a combination of central altitude and amplitude, the linear fit between the time-window-averaged signal and the theoretical molecular attenuated backscatter profile is performed. In order to reject those range windows still affected by aerosol loads, a test is performed to check for the presence of coherent structures therein. More specifically, the Breusch-Godfrey test (BG test; Breusch, 1978) is applied to calculate the autocorrelation in fit residuals. The windows associated with the p-value of the BG test > 0.05 are rejected (QC.CAL1). From the ensemble of retained windows, the molecular window selected for the calibration is the one maximising a metric (M_{Ray}) defined as follows:

$$M_{Ray} = \frac{adjR^2 + (1 - |b|)}{std(b)} \quad \text{(S3)}$$

where $adjR^2$ and b represent the adjusted R^2 and the intercept of the linear fit, respectively, and std(b) is the standard deviation of b over the ensemble of potential molecular windows. In particular, the adjusted R^2 is calculated as:

$$adjR^2 = 1 - \frac{(1 - R^2)(n-1)}{(n-k-1)} \quad \text{(S4)}$$

where n is the number of data points within the molecular window and k is the number of predictor variables.
The following quality controls are then further performed:

- the slope of the linear fit must be positive and the intercept nearly 0 (QC.CAL.2);
- the autocorrelation (BG test) and the cumulative sign of fit residuals at the window borders (± 200 m from each border) must be > 0.05 and < 0, respectively (QC.CAL.3). This quality control is effective in filtering the range windows that lie over an undetected aerosol layer but are associated with a misleading robust linear regression with the molecular profile.

If one of these QCs is not met, the night is rejected for calibration purposes, and the process continues using data from the following night.

b) C_L computation. Once the molecular window is selected, the backward Klett inversion (Klett, 1985) converts the time-window-averaged ALC signal into the total attenuated β_{att} profile. Note that the sign correction in the Klett algorithm reported by Speidel and Vogelmann (2023) was already introduced in the ALICENET procedure since the beginning of its activities. The C_L is derived as (Wiegner and Geiβ, 2014):

$$C_L = median\left(\frac{P(r)\frac{r^2}{Ovl}(r)}{\beta_{att}(r)}\right) \quad \text{(S5)}$$

where P(r) r^2 / Ovl is the time-window-averaged, range- and overlap-corrected ALC signal, and the median is calculated along the identified molecular range-window.

Two further quality controls are then performed at this stage:

- calibration coefficients associated with relative uncertainty E_{CL} > 40% are rejected (QC.CAL.4). The calibration coefficient relative uncertainty is defined as follows:

$$E_{CL} = \frac{err\left(C_L^{slope}\right)}{C_L^{slope}} + \frac{std\left(C_L\right)}{median\left(C_L\right)} \quad \text{(S6)}$$

  In the first term, C_L^{slope} represents the slope of the fit between the ALC signal and the theoretical molecular backscatter profile within the molecular range-window, and err(C_L^{slope}) the standard error of the slope. In the second term, median(C_L) and std(C_L) represent the median and the standard deviation of the calibration coefficient as derived in Wiegner and Geiβ (2014) within the molecular range-window, respectively;

- calibration coefficients leading to a negative AOD are rejected (QC.CAL.5). This quality control effectively filters those C_L associated with calibration windows containing residual aerosols. In such cases, the aerosol extinction coefficient resulting from the Klett inversion can assume slightly negative values and lead to a negative sign of the AOD.

Determination of C_L can be hampered in periods of unfavourable atmospheric conditions or high aerosol loads in the middle troposphere, where the calibration window is generally selected. Moreover, the C_L coefficients of different ALICENET systems followed a seasonal cycle (see Fig. 5 and related text) as observed in other European ALC networks. Currently, the C_L values operationally applied in ALICENET inversions are interpolated in time using a non-parametric regression of the C_L coefficients. More specifically, a locally weighted smoothing (Loess) fit with a time span > 1 year (tunable) is used.

S4 Retrieval of aerosol properties

S4.1 Aerosol optical properties

In ALICENET, the aerosol backscatter (β_p) and extinction (α_p) are retrieved from Eq. 1 using the forward Klett inversion. To this purpose these two unknowns in Eq. 1 are linked one to the other through the functional relationship $\alpha_p=\alpha_p(\beta_p)$ derived using pre-computed simulations from a continental aerosol model (Dionisi et al., 2018). Operatively, an iterative procedure is applied within the forward Klett inversion to derive $\beta_p(r)$ and $\alpha_p(r)$ vertical profiles as follows:

1. the procedure starts from a first-guess, vertically-constant Lidar Ratio (LR) profile of 38 sr, this being similar to the value used in the NASA-CALIPSO inversion at 1064 nm for clean/polluted continental aerosol (Omar et al., 2009);
2. the LR profile is then updated at each iteration based on the $\alpha_p=\alpha_p(\beta_p)$ functional relationship;
3. the iterations stop when convergence on the final β_p profile is reached. The established requirement is that the vertically integrated aerosol backscatter difference in two successive iterations keeps < 0.0025 m^{-1} sr^{-1}.

The iterative procedure can 'adjust' the first-guess, vertically constant LR profile according to the actual aerosol stratification. An example of the 'adjusted', vertically-variable LR profiles is shown in Fig. S3a, referring to the same period addressed in Fig. 6. It is worth mentioning that a main advantage of the variable-LR method is the fact that it is independent of ancillary (e.g., sunphotometer) data and a-priori assumptions (e.g., the actual LR value to be used), thus allowing an automatic, homogeneous retrieval of aerosol properties in different sites and periods. As reported in the main text (Fig. 7) and further shown in Dionisi et al. (2018), the ALICENET-retrieved aerosol optical properties were found in good agreement with independent sunphotometer data in different sites. A comparison of the performances of the adjusted-LR and fixed-LR approaches was also conducted by Dionisi et al. (2018) using ALC data from various stations. In brief, the authors found a good agreement between sunphotometer and ALC-based AOD using both the iterative procedure and a fixed LR of 38 sr, and larger discrepancies using a fixed LR of 52 sr, regardless of the site location. As an example, for the same period presented in Fig. 6, we show in Fig. S3b the comparison of the AOD retrieved with both ALICENET processing and fixed-LR values (chosen as in Dionisi et al., 2018) and the reference AERONET L2 AOD.

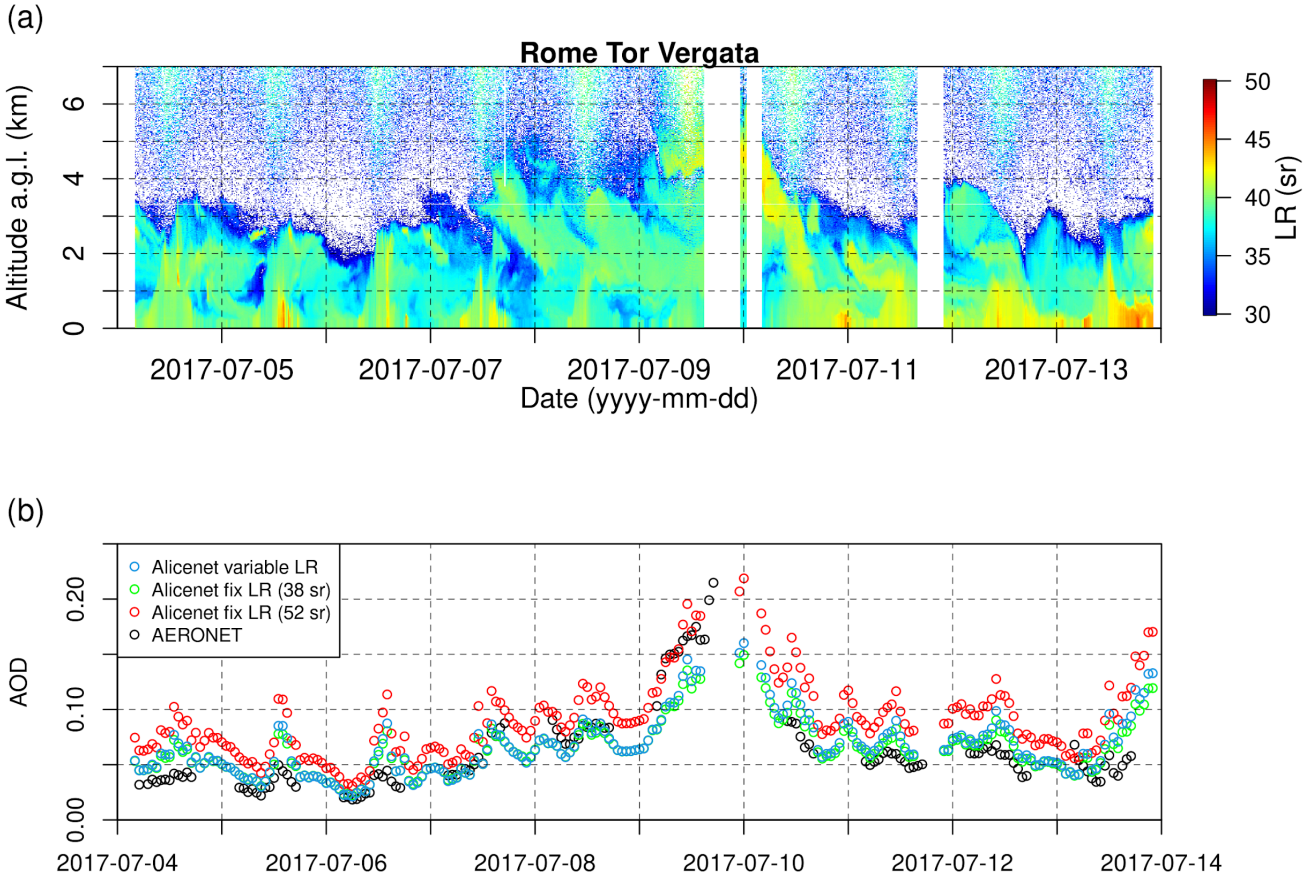

Figure S3: (a) Variable Lidar Ratio (LR) profiles derived within the ALICENET processing on the CHM15k operating in Rome - Tor Vergata in the same period presented in Fig. 6; (b) AOD retrieved with both ALICENET processing and fixed-LR values (chosen as in Dionisi et al., 2018) compared to reference AERONET L2 data.

In the main text, we evaluated the overall performances of the ALICENET retrieval of aerosol optical properties using multiannual datasets of three ALICENET systems located in very different environments (Fig. 7). Here, we further explore the reasons for the main discrepancies. In particular, Fig. S4 shows the same data as Fig. 7, with the separation of data pairs based on the photometer-derived Ångstrøm Exponent. It shows that most deviations from the 1:1 line are associated with coarse-mode dominated aerosol types (AE < 0.5, red), likely due to desert dust or sea-salt particles, thus deviating from the continental aerosol model assumed for the derivation of the functional relationships used in the ALC data inversion.

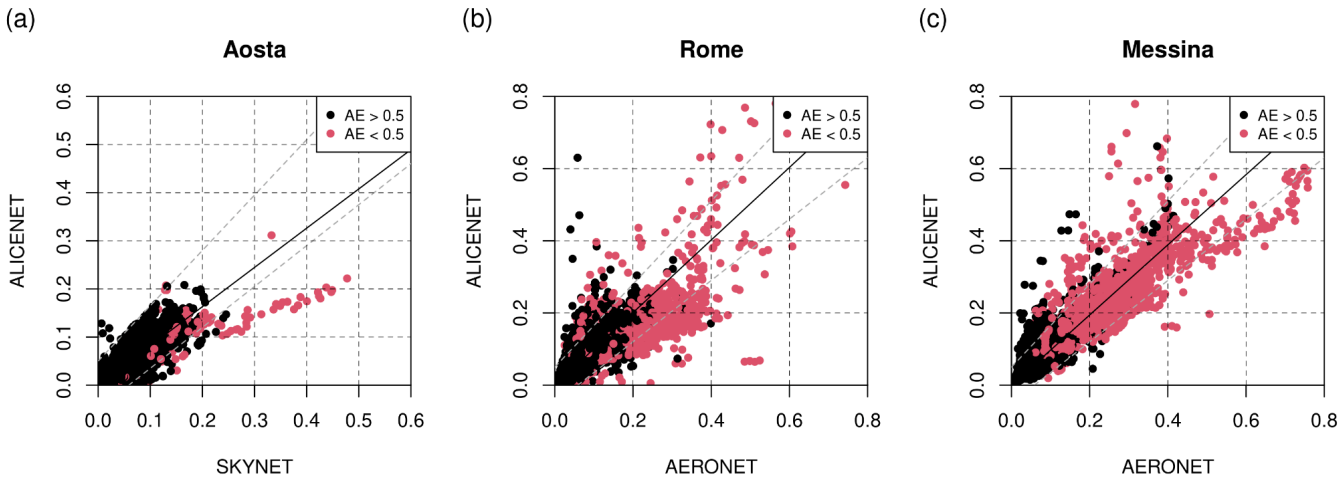

Figure S4: Same as Figure 7, but separating data pairs associated with a sunphotometer-derived Ångstrøm Exponent (AE) < 0.5 (red) and > 0.5 (black).

S4.2 Aerosol physical properties

In the main text (Sect. 3.3.2), we discussed the need to estimate 'dry' aerosol mass concentrations from ALC-based 'wet' aerosol profiles when aiming at the direct comparison with reference in-situ instrumentation. In such cases, we derive the dry aerosol mass concentrations, M_p^{dry}, from the ALC (wet) aerosol mass concentrations, M_p, following Adam et al. (2012):

$$M_p^{dry} = \frac{M_p^{dry}}{1+\frac{1}{\rho_d}\left(GF^3-1\right)} \quad \text{(S7)}$$

where

$$GF = \left(1 - \frac{RH}{100}\right)^{-\gamma} \quad \text{(S8)}$$

is the hygroscopic growth factor, and RH is the ambient relative humidity. The values of the dry aerosol density ρ_d and the γ exponent depend on the aerosol mixture under investigation and are the main sources of uncertainty in the aerosol mass retrieval (Adam et al., 2012; see also main text, Sect. 3.3.3). Their accuracy strongly depends on the possibility to identify the actual, dominant aerosol type, e.g., using the PLC depolarisation information and/or model data.

An example of this RH-correction was reported in Fig. 8 (see main text), which shows the comparison between the ALICENET-derived M_p^{dry} in the sounded altitude range 3500 ± 200 m a.s.l. and the in-situ PM_{10} measurements from an OPC operating at the high altitude (3500 m a.s.l.) station Testa Grigia - Plateau Rosa (data courtesy of Stefania Gilaroni CNR-ISP) in June 2022. The aerosol mass concentrations were retrieved from the CHM15k operating in Aosta, which is about 35 km apart from Testa Grigia (see Fig. S5).

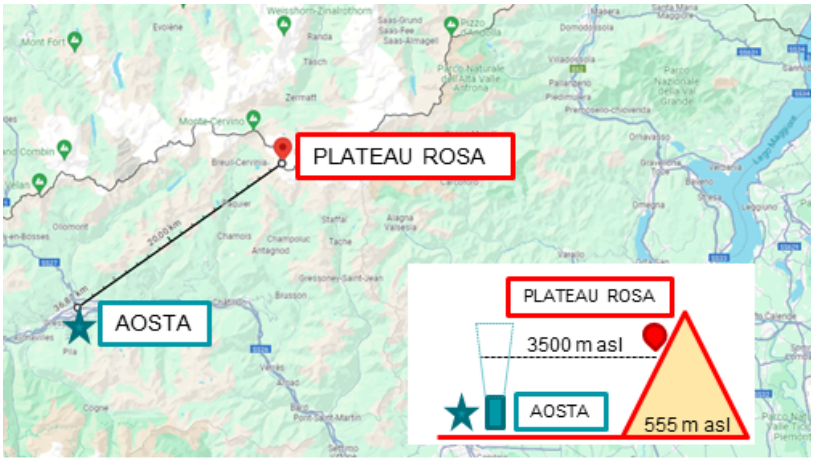

Figure S5: Map with the locations of the Aosta and Testa Grigia - Plateau Rosa stations (35 km apart). A scheme with the station altitudes is also reported in the bottom-right corner. Background Map credits: © Google Maps.

In that case, we set $\gamma = 0.2$ in the presence of continental, hygroscopic aerosols (D'Angelo et al., 2016) and $\gamma = 0$ (i.e., $M_p^{dry} = M_p$) in the presence of dust, hydrophobic particles (Barnaba et al., 2010). The aerosol type was assessed through the linear volume depolarisation ratios (δ_v) profiles of a co-located PLC, assuming that aerosol mixtures associated with $\delta_v < (>)$ 15% are dominated by continental (dust) particles. The RH at the relevant altitude was extracted from the dataset of the high-resolution atmospheric model MERIDA (Bonanno et al., 2019). During the period addressed in Fig. 8, at the altitude of Testa Grigia - Plateau Rosa the simulated RH ranged from 16% to 98%, and the measured δ_v from 0.4% to 27%. In Fig. S6a we further show the same data in Fig. 8, including RH-non-corrected (wet, blue bullets) and RH-corrected (dry, red bullets) aerosol mass concentrations as retrieved by ALICENET. The median difference between the ALC-based wet/dry aerosol mass concentrations and the OPC PM_{10} measurements was evaluated as a function of RH in Fig. S6b. It shows the median differences between ALC- and OPC-based aerosol mass concentrations per RH bins, with dry values around zero. On average, the hygroscopic correction reduced the difference between ALC and OPC mass estimates. However, the large horizontal distance between Aosta and Testa Grigia - Plateau Rosa and the uncertainty of the ALICENET aerosol volume retrieval in dust conditions strongly complicate the evaluation of this correction.

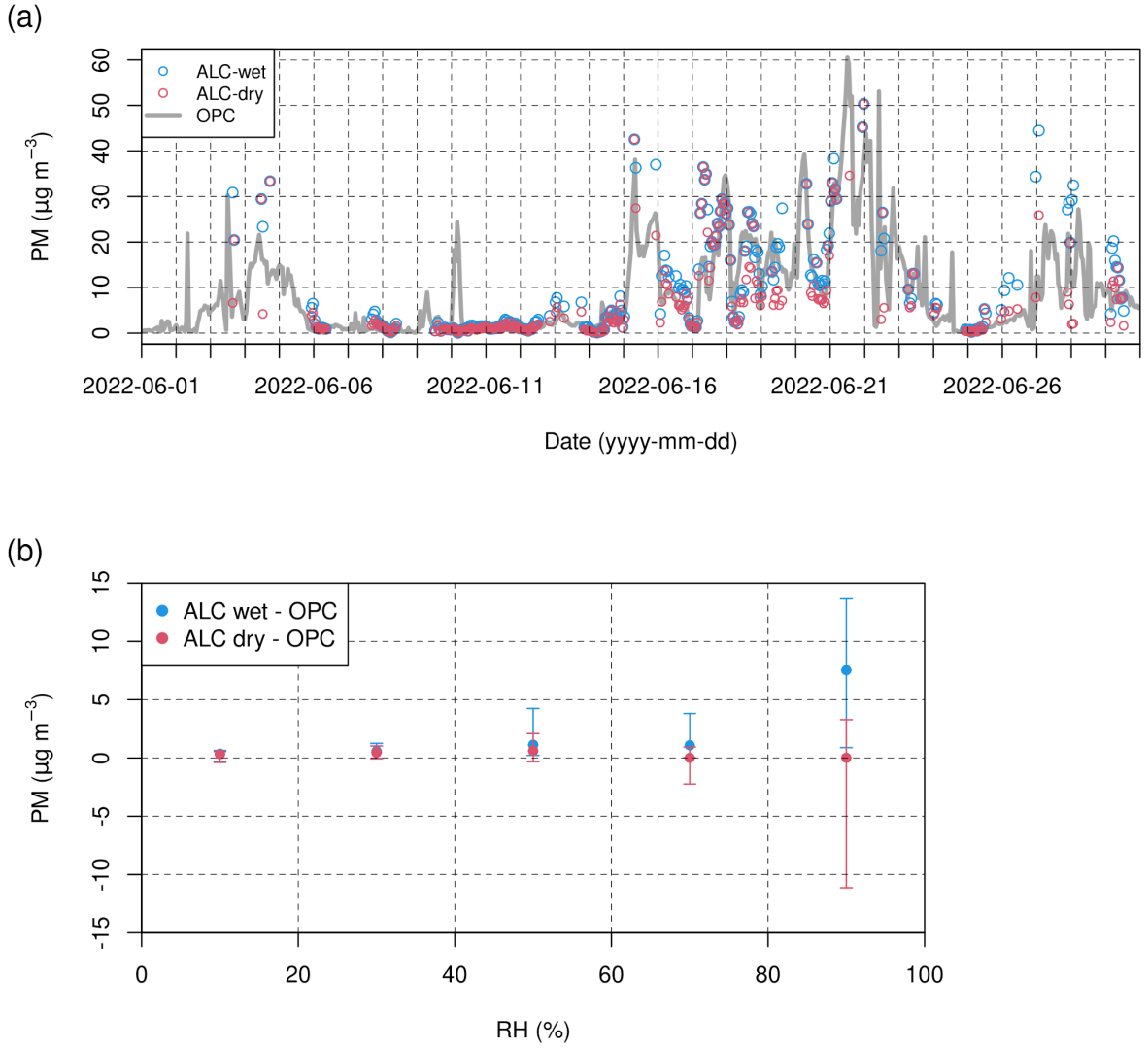

Figure S6: (a) Same as Figure 8, but including both wet (blue bullets) and dry (red bullets) aerosol mass concentrations as retrieved by ALICENET; (b) Median differences (points) and 25–75 percentiles (bars) between ALC- and OPC-based aerosol mass concentrations per RH bins (0-20%, 20-40%, 40-60%, 60-80%, 80-100%) for data reported in panel (a).

S5 The ALICENET ALADIN tool for the automatic detection of aerosol layers

The monitoring capability of ALCs offers the opportunity to have continuous, accurate information on the aerosol vertical distribution. While several tools are already available for the ALC-based detection of the atmospheric boundary layer and mixed layer heights (e.g., Kotthaus et al., 2020, 2023), a specific need in the Italian context was also the further automatic identification of lofted aerosol layers. We thus developed an original tool (ALADIN: Aerosol LAyer DetectIoN) to identify main aerosol stratifications from ALC/PLC L2 profiles. The aerosol layers targeted by ALADIN are: 1. the Continuous Aerosol Layer (CAL), i.e., the layer continuously dominated by aerosols from the ground level up to its upper boundary; 2. the Mixed Aerosol Layer (MAL), this being a CAL sublayer within which particles are mixed by turbulent fluxes; 3. Elevated Aerosol Layers (EALs), i.e., lofted aerosol layers that are located above the MAL and either within or above the CAL. The ALADIN procedures for detecting CAL, MAL, and EALs are described hereafter and summarised in Fig. S7.

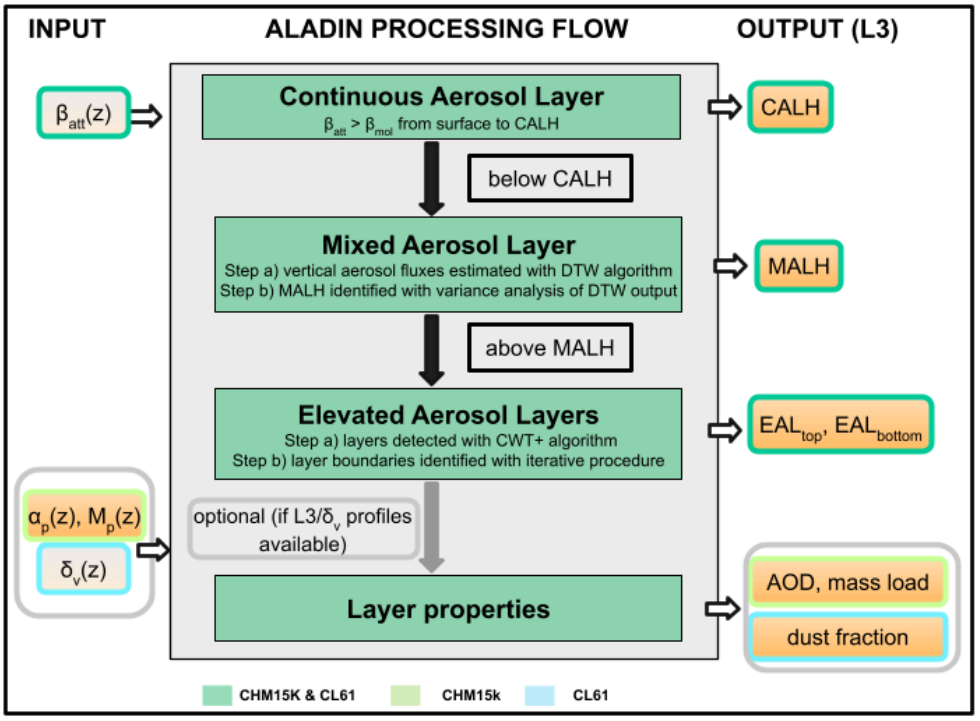

Figure S7: Scheme of the ALADIN (Aerosol LAyer DetectIoN) processing flow from the input total attenuated backscatter (β_{att}) profiles to L3 output products. As in Fig. 2, the different box contour colours are used to indicate products valid for CHM15k ALCs (light green), CL61 PLCs (cyan), or both (dark green) systems. Relevant ALICENET L3 output products include the Continuous Aerosol Layer Height (CALH), the Mixed Aerosol Layer Height (MALH), and the top and bottom boundaries of Elevated Aerosol Layers (EAL_{top} and EAL_{bottom}, respectively). Optionally, if L3 profiles of aerosol properties (such as aerosol extinction, α_p, and mass concentrations, M_p) and/or volume linear depolarisation ratio (δ_v) profiles are available, specific mean properties of the aerosol layers can be derived, such as the layer Aerosol Optical Depth (AOD), mass load, or dust fraction.

1. The CAL height (CALH) is derived from cloud-screened, denoised β_{att} profiles averaged at 30 min resolution. It is defined as the altitude of the layer extending from the surface, in which $\beta_{att} > \beta_{mol}$ for at least 98% of its extension. The CALH search is performed in the vertical range 225-7000 m a.g.l.

2. The MAL is identified through a technique highlighting regions where aerosols are mixed by vertical turbulent fluxes. The procedure comprises two steps: a) the estimation of vertical aerosol fluxes and b) the analysis of the associated variance.

a) We estimate vertical aerosol fluxes by applying a Dynamic Time Warping algorithm (DTW, Giorgino et al., 2009) to a sequence of β_{att} profiles at relatively high (1-min) resolution. In brief, this algorithm computes the local stretch or compression to be applied to the β_{att} sequence to link each profile to the following one optimally. An example of the output field of the DWT procedure, w_{DTW}, is given in Figure S8a for the same episode addressed in Fig. 6. The variable w_{DTW} can be interpreted as the local vertical displacement of the aerosol-loaded air parcels (i.e., similar to a vertical velocity), therefore the region near the surface where it rapidly changes in sign and magnitude highlights where the mixing is acting.

b) The variance analysis of w_{DTW} allows us to identify the MAL height (MALH). First, we compute the standard deviation of w_{DTW} (σ_w) over 30 min intervals as generally done in Eddy-Covariance analysis (Aubinet et al., 1999). The MAL height at time t, MALH(t), is then defined as the height of the first σ_w local minima which:

- lies within MALH(t-Δt) - 600 m and MALH(t-Δt) + 1200 m during the morning, and MALH(t-Δt) + 600 m and MALH(t-Δt) - 1200 m during the afternoon, with Δt=30 min;
- minimises the following metric:

$$M_{mal} = \left| z_{min} - MALH(t - \Delta t) \right| + \frac{1}{median(\sigma_w)} \quad \text{(S9)}$$

where z_{min} denotes the height of the σ_w local minima, and the median is calculated along the vertical range 225 m - z_{min}.

The σ_w field and the identified MAL heights are shown in Fig. S8b (same period as Fig. 6).

The search of MALH is performed:

- below CALH and within site- and season-dependent maximum and minimum values defined by the user. For example, in Rome-Tor Vergata a maximum height of 3500 (2500) m is set during summer (winter). In general, the MAL lower limit must be higher than the height of the ALC blind overlap region, which is approximately 225 m for CHM15k systems and a few tens of metres for CL61 systems;
- from 1 hour before sunrise to 1 hour after sunset (the site- and season-dependent sunrise/sunset hours are calculated using the Michalsky algorithm (Michalsky, 1988)).

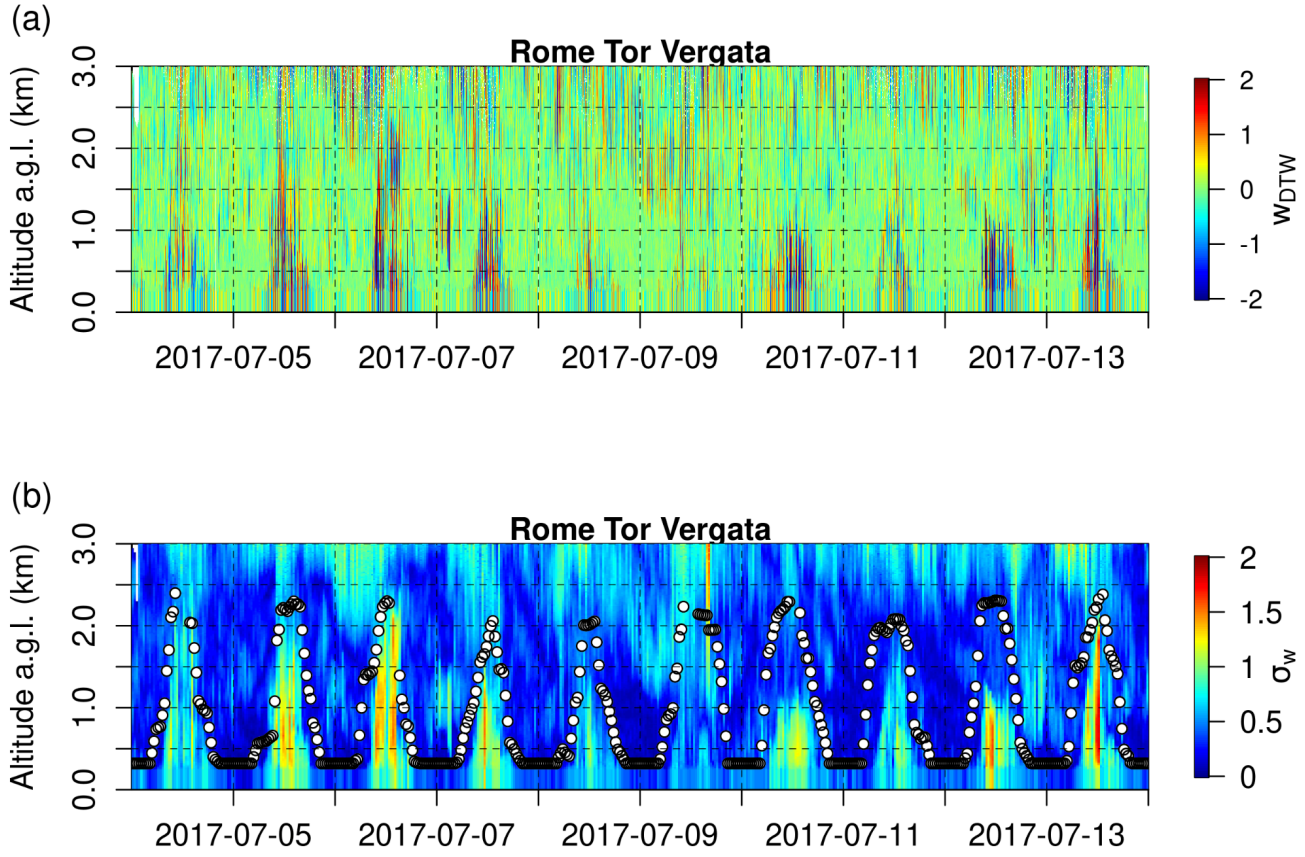

Figure S8: (a) Output field of the Dynamic Time Warping algorithm (w_{DTW}) applied to the β_{att} profiles of the CHM15k operating in Rome-Tor Vergata in the same period presented in Fig. 6, and (b) 30-min standard deviation of w_{DTW} (σ_w) and corresponding Mixed Aerosol Layer (MAL) heights (white points) identified by the ALADIN procedure.

3. The EALs are detected from cloud-screened and denoised β_{att} profiles averaged at 30 min resolution. The procedure, which includes specific quality controls (QC.EAL, see also Table S1), is made of two steps: a) the detection of the presence of elevated layers, and b) the identification of their top and bottom boundaries.

a) We identify lofted aerosol layers using the Continuous Wavelet Transform (CWT) algorithm developed by Du et al. (2006). This algorithm, referred to as CWT+, has the advantage of discriminating signal peaks attributable to aerosol layers from noise spikes by analysing both β_{att} and CWT coefficients. The peak search is performed from MALH up to 7 km a.g.l.

b) we derive the top and bottom boundaries (EALtop and EALbottom, respectively) with an iterative technique for each detected aerosol layer. Operatively, an ensemble of potential bottom and top boundaries is considered, and for each bottom-top combination the following metric is calculated:

$$M_{eal} = \frac{\int \beta_{att}(r)dr}{\int \beta_{ref}(r)dr} + Perc\left(\beta_{att} > \beta_{ref}\right) + G_{border} + CWT_{border} \quad \text{(S10)}$$

where β_{ref} denotes a 'reference' total attenuated backscatter profile, the integrals are calculated along the bottom-top range, Perc represents the percentage of points with $\beta_{att} > \beta_{ref}$ along the bottom-top range, G_{border} denotes the normalised mean gradients of β_{att} and CWT_{border} the normalised mean CWT coefficients along the vertical ranges $EAL_{top} \pm 90$ m and $EAL_{bottom} \pm 90$ m.

The EAL vertical range is selected as the top-bottom combination maximising the M_{eal} metric.

It is worth highlighting that, with this approach, the choice of β_{ref} depends on the application. Molecular attenuated backscatter profiles are used as a reference when the aim is to detect aerosol layers with respect to a clean atmosphere. In contrast, 'climatological' site-dependent β_{att} profiles, such as those derived from our multiannual datasets, are used to identify anomalous aerosol layers concerning the typical aerosol conditions.

Finally, three conditions (QC) must be fulfilled to identify an EAL:

- within the layer it should be Perc($\beta_{att} > \beta_{ref}$) > 90% (QC.EAL.1) and $\int \beta_{att}(r)\, dr > \int \beta_{ref}(r)\, dr$ (QC.EAL.2);
- it should be $G_{border} < 0$ at the EAL top, $G_{border} > 0$ at the EAL bottom, and $CWT_{border} < 0$ at both boundaries (QC.EAL.3).

When corresponding L3 inversions or PLC linear volume depolarisation ratio (δ_v) profiles are available, mean properties of the different aerosol layers can also be derived, such as the layer AOD and mass load or the mean fraction of irregular (generally dust) particles within the layer, F_d. In the last case, we exploit the PLC δ_v profiles as follows (Tesche et al., 2009):

$$F_d = median\left(\frac{(\delta_v - \delta_{nd})(1+\delta_d)}{(\delta_d - \delta_{nd})(1+\delta_v)}\right) \quad \text{(S11)}$$

where δ_d and δ_{nd} are the typical linear volume depolarisation ratios of dust and non-dust particles, respectively, and the median is calculated within the layer boundaries.

S6 Summary of quality controls within the overall ALICENET processing chain

In Table S1, we summarise the Quality Controls (QCs) discussed above and associated with the ALICENET processing steps (see also Fig. 2), namely the overlap correction (QC.OVL), the absolute calibration (QC.CAL), and the ALADIN detection of elevated aerosol layers (QC.EAL).

ALICENET processing step (Supplement Section)	**Quality Controls (QCs)**
Overlap correction (S2)	QC.OVL1: it filters out of the ensemble unphysical overlap corrections QC.OVL2: it ensures that the overlap model is derived over a statistically significant dataset QC.OVL3: it ensures that the temperature-dependent overlap model is derived over an ensemble spanning a representative range of temperatures
Absolute calibration (S3)	QC.CAL1: it filters potential calibration (molecular) windows that are affected by the presence of aerosol layers within their boundaries QC.CAL2: it ensures that the parameters of the fit between the ALC signal and the theoretical molecular profile lie within physical ranges QC.CAL3: it ensures that the calibration window is not located over a homogeneous aerosol layer QC.CAL4: it filters calibration coefficients that are associated with unacceptable relative uncertainties QC.CAL5: it filters calibration coefficients that lead to a negative aerosol optical depth in the vertical range 0-4 km a.g.l.
ALADIN detection of elevated aerosol layers (S5)	QC.EAL1: it ensures that the percentage of points exceeding a reference profile within the EAL top-bottom range is greater than 90% QC.EAL2: it ensures that the integrated aerosol backscatter within the EAL top-bottom range is greater than the one obtained with the reference profile QC.EAL3: it ensures that the β_{att} gradient and CWT coefficients at the layer borders are consistent with the presence of an aerosol layer

Table S1: Summary of Quality Control (QC) criteria applied within the different steps of the ALICENET processing chain.

When investigating their temporal and vertical variability over the long term, ALICENET aerosol products are subject to additional Quality Assurance (QA) criteria.